AIAA JOURNAL
Vol. 33, No. 9, September 1995

# Sound Propagation Simulations Using Lattice Gas Methods

Yasushi Sudo* and Victor W. Sparrow†
*Pennsylvania State University, University Park, Pennsylvania 16802*

**A new lattice gas model for one-dimensional sound propagation has been recently proposed by the authors. In this paper, its extension to a sound propagation model in a two-dimensional square lattice is discussed. A variation on standard splitting methods is used to extend the formulation developed for the one-dimensional model to obtain a two-dimensional model. In arbitrary directions of propagation the method is at least second-order accurate. However, the accuracy is greatly increased for narrow angle propagation along the coordinate axes.**

## Nomenclature

$C$ = dimensionless sound speed
$c$ = sound speed
$e_1$ = unit vector in the $+x$ direction
$e_2$ = unit vector in the $+y$ direction
$I$ = unit dyadic or unit matrix
$p$ = acoustic pressure
$p_j$ = acoustic pressure of the $j$th velocity state
$p_j^{(l)}$ = $l$th-order expansion coefficient of $p_j$ about $\epsilon$
$v$ = scalar acoustic particle velocity
$\boldsymbol{v}$ = acoustic particle velocity
$\boldsymbol{v}_j$ = acoustic particle velocity of the $j$th velocity state
$\boldsymbol{v}_j^{(l)}$ = $l$th-order expansion coefficient of $\boldsymbol{v}_j$ about $\epsilon$
$Z$ = characteristic impedance of the fluid medium
$\Delta t$ = sampling time
$\Delta x$ = sampling distance in the $x$ direction
$\Delta y$ = sampling distance in the $y$ direction
$\delta_{i,j}$ = Kronecker's delta
$\epsilon$ = expansion parameter for the continuum limit
$\nu_j$ = wave speed value of the $j$th velocity state
$\rho$ = acoustic density
$\rho_0$ = ambient density
$\tau$ = scaling factor of the sampling time
$\chi$ = scaling factor of the sampling distance

## Introduction

LATTICE gas models have been developed mainly for fluid dynamic systems.[1,2] The key idea of lattice gas models is to start from a dynamic system in a discrete space and time instead of starting from a discretization of a partial differential equation. The temporal evolution rule is designed so that the discrete system may become a desired model system in the continuum limit. This approach assures that lattice gas models are stable, simple, and local, and such properties ease implementations on massively parallel computers. Because of these nice properties, several attempts to develop lattice gas models for systems other than fluid dynamics systems have been made.[3–5]

The main concern of this paper is lattice gas models for sound propagation. Frisch et al.[2] pointed out that lattice gas fluid models include sound propagation in their small perturbation limit. Margolus et al.[6] showed sound wave propagations in a lattice gas fluid model in a numerical simulation. Rothman[7] applied this idea to a lattice gas model for seismic $P$ waves. Huang et al.[8] extended Rothman's model to the case for inhomogeneous media. Chen et al.[9] performed a theoretical analysis of the sound propagation of a lattice gas fluid model. Lavallée[10] undertook an additional theoretical analysis. Chen et al.[11] proposed a lattice gas model that directly simulates a linear wave system not as a small perturbation limit of fluid systems. Krutar et al.[12] and Numrich et al.[13] modified Chen et al.'s model and performed massively parallel computations of underwater sound propagation. From a different point of view from the preceding models, we have recently proposed a new lattice gas model for one-dimensional sound propagation.[14]

In our one-dimensional lattice gas wave model, we have started from a lattice gas model for a one-way wave system. Lattice gas particles of this model are assumed to move with either unit or zero velocity. The temporal change of the particle velocity is given in an appropriate way and is assumed to be periodic in time. Let $N$ be the period of the temporal change in the instantaneous velocity of the lattice gas particle. A positive integer $M$ was used to express the number of the unit velocity cases during the period $N$ change of the instantaneous velocity. It was shown that the dimensionless wave speed $C$ is equal to $M/N$. From the definition, one has $C \leq 1$. Corresponding to this period $N$ change of velocity, we have introduced $N$ different velocity states at each space point. We have shown that the average number of the lattice gas particles in the $N$ velocity states satisfies a one-way wave equation in the continuum limit and that there is no truncation error in this model. Combining the right-going wave model and the left-going wave model, we have obtained a lattice gas model for one-dimensional sound wave propagation.

In our one-dimensional sound propagation model, the $N$ different velocity states are arranged so that the unit velocity states for right-going particles and those for left-going particles are the same. Hence, those unit velocity states correspond to unit speed propagations of sound waves in both $\pm x$ directions. The zero velocity states for both right-going and left-going lattice gas particles are also assumed to be the same. These zero velocity states correspond to a nonpropagation state. To express the difference of each velocity state, the wave speed values $\nu_j$ are defined as

$$\nu_j = \begin{cases} 1 & \text{(unit speed propagation)} \\ 0 & \text{(no propagation)} \end{cases} \qquad (j = 1, \ldots, N) \quad (1)$$

where $\nu_j$ represents the motion of the particles in the $j$th velocity states.

In our one-dimensional sound model, the acoustic pressure $p(x, t)$ and the scalar acoustic particle velocity $v(x, t)$ at position $x$ and time $t$ are defined by the averages of those in $N$ different velocity states as

$$p(x, t) = \frac{1}{N} \sum_{j=1}^{N} p_j(x, t) \qquad (2)$$

Received Oct. 15, 1993; presented as Paper 93-4404 at the AIAA 15th Aeroacoustics Conference, Long Beach, CA, Oct. 25–27, 1993; revision received Nov. 8, 1994; accepted for publication Nov. 15, 1994. 

*Graduate Student, Graduate Program in Acoustics; currently Technical Official, Fifth Research Center, Japan Defense Agency, 3-13-1 Nagase, Yokosuka-shi, Kanagawa 239, Japan. Student Member AIAA.

†Assistant Professor, Graduate Program in Acoustics, 157 Hammond Building. Member AIAA.

and

$$v(x,t) = \frac{1}{N}\sum_{j=1}^{N} v_j(x,t) \tag{3}$$

One can interpret $p_j$ and $v_j$ as the number of lattice gas particles and the momentum in the $j$th state, respectively. However, as we have indicated previously, if we treat the lattice gas particles as information carriers and allow the field variables $p_j$ and $v_j$ to be real numbers, it is simple to implement the boundary conditions. According to this interpretation, we can imagine the following simple picture.

There are two lattice gas particles in each velocity state at each lattice node. One of them has a tendency to move in the $+x$ direction and the other in the $-x$ direction. When the value of the wave speed function of the state is one, both particles move to the next velocity states of nearest neighbor nodes of opposite directions. The amounts of the physical quantities carried by each lattice gas particle are $[p_j(x,t) \pm Zv_j(x,t)]/2$ and $[v_j(x,t) \pm p_j(x,t)/Z]/2$ for the $j$th state, where $Z = \rho_0 c$ is the characteristic impedance. The new values of the field variables are determined by simply adding the contribution carried by the lattice gas particle from the left nearest neighbor node and that from the right nearest neighbor node. The signs correspond to the particle moving in the $+x$ direction and that in the $-x$ direction, respectively. When the value of the wave speed value is zero, both particles move to the next velocity states of the same position. The physical quantities are simply handed to the next velocity state. In this way, the number of the lattice gas particles in each state is always two.

According to the preceding interpretation, the temporal evolutions of $p_j(x,t)$ and $v_j(x,t)$ are expressed as

$$\begin{aligned} p_j(x,t+1) &= \delta_{\nu_{j\ominus 1},0}\, p_{j\ominus 1}(x,t) \\ &\quad + \delta_{\nu_{j\ominus 1},1}\left\{\tfrac{1}{2}[p_{j\ominus 1}(x-1,t) + Zv_{j\ominus 1}(x-1,t)]\right. \\ &\quad \left. + \tfrac{1}{2}[p_{j\ominus 1}(x+1,t) - Zv_{j\ominus 1}(x+1,t)]\right\} \qquad (j = 1,\ldots,N) \end{aligned} \tag{4}$$

and

$$\begin{aligned} v_j(x,t+1) &= \delta_{\nu_{j\ominus 1},0}\, v_{j\ominus 1}(x,t) \\ &\quad + \delta_{\nu_{j\ominus 1},1}\left\{\tfrac{1}{2}\left[v_{j\ominus 1}(x-1,t) + \frac{1}{Z}p_{j\ominus 1}(x-1,t)\right]\right. \\ &\quad \left. + \tfrac{1}{2}\left[v_{j\ominus 1}(x+1,t) - \frac{1}{Z}p_{j\ominus 1}(x+1,t)\right]\right\} \qquad (j = 1,\ldots,N) \end{aligned} \tag{5}$$

The notation $(j \ominus 1)$ is used to express

$$j \ominus 1 = \begin{cases} \mathrm{mod}(j-1,N) & \text{for} \quad \mathrm{mod}\,(j-1,N) \neq 0 \\ N & \text{for} \quad \mathrm{mod}\,(j-1,N) = 0 \end{cases} \tag{6}$$

The distance and the time are nondimensionalized by the sampling time and the sampling distance.

In this paper, we use the same interpretation as the one-dimensional model. That is, the lattice gas particles are information carriers moving in a lattice according to given rules. The field variables are real valued, represented as floating point numbers in computers.

## Lattice Gas Sound Propagation Model in a Two-Dimensional Square Lattice

### Basic Formulation

In this subsection we explain the basic idea of our approach to extend the one-dimensional sound propagation model to the two-dimensional square lattice case. For simplicity, the lattice is assumed to be uniform and the space and the time are nondimensionalized using the sampling distance $\Delta x = \Delta y\ (\equiv \Delta r)$ and the sampling time $\Delta t$.

At the end of the previous section, a simple lattice gas picture of Eqs. (4) and (5) was presented. It is not difficult to extend this simple picture to a two-dimensional square lattice case. Let's imagine four lattice gas particles in each velocity state at each lattice node. These particles have tendencies to move in the $+x$, $-x$, $+y$, and $-y$ directions, respectively. Now that we have two possible directions of motion, we assume three types of velocity states.

In the first type the velocity state corresponds to unit speed propagations along the $x$ axis. In this case, the two lattice gas particles with motion tendencies in $\pm x$ directions move to the next states in the nearest neighbor nodes of the $\pm x$ directions. They carry the acoustic pressure and the $x$ component of the acoustic particle velocity in the velocity state. To determine the amount, we use a similar method to the one-dimensional case. The remaining lattice gas particles move to the next velocity state of the same position. The latter particles carry the $y$ component of the acoustic particle velocity of the velocity state.

In the second type of velocity state, the two particles with tendencies of motion in $\pm y$ directions move to the next velocity state in the nearest neighbor nodes in the $\pm y$ directions. The acoustic pressure and the $y$ component of the acoustic particle velocity of the state are carried by them. The remaining particles move into the next velocity state of the same lattice node and carry the $x$ component of the acoustic particle velocity.

The third type is a nonpropagation state. All of the lattice gas particles in this state move into the next velocity state of the same lattice node. The physical quantities are also carried into the next state.

In this way, the number of lattice gas particles in each velocity state is always four. The new values of the field variables are determined simply by adding all of the contributions carried by the lattice gas particles.

To implement the preceding idea, the wave speed values $\nu_j$ are modified to

$$\nu_j = \begin{cases} 0 \text{ (no propagation)} \\ 1 \text{ (unit speed propagation along } x \text{ axis)} \\ \qquad\qquad\qquad\qquad (j = 1,\ldots,N) \\ 2 \text{ (unit speed propagation along } y \text{ axis)} \end{cases} \tag{7}$$

In the following part of this paper, the number of the unit speed propagation states along either the $x$ or $y$ axes is expressed by a positive integer $M$. Hence, from the definition of the $\nu_j$, one has

$$M = \sum_{j=1}^{N} \delta_{\nu_j,1} = \sum_{j=1}^{N} \delta_{\nu_j,2} \tag{8}$$

From the preceding picture of the lattice gas particles in a two-dimensional square lattice, using Eq. (7)'s $\nu_j$, Eqs. (4) and (5) lead to the following expression for the temporal evolution rules of the field variables:

$$\begin{aligned} p_j(\boldsymbol{x},t+1) &= \delta_{\nu_{j\ominus 1},0}\, p_{j\ominus 1}(\boldsymbol{x},t) \\ &\quad + \sum_{l=1}^{2} \delta_{\nu_{j\ominus 1},l}\left\{\tfrac{1}{2}[p_{j\ominus 1}(\boldsymbol{x}-\boldsymbol{e}_l,t) + Z\boldsymbol{e}_l\cdot\boldsymbol{v}_{j\ominus 1}(\boldsymbol{x}-\boldsymbol{e}_l,t)]\right. \\ &\quad \left. + \tfrac{1}{2}[p_{j\ominus 1}(\boldsymbol{x}+\boldsymbol{e}_l,t) - Z\boldsymbol{e}_l\cdot\boldsymbol{v}_{j\ominus 1}(\boldsymbol{x}+\boldsymbol{e}_l,t)]\right\} \\ &\qquad\qquad (j = 1,\ldots,N) \end{aligned} \tag{9}$$

and

$$\begin{aligned} \boldsymbol{v}_j(\boldsymbol{x},t+1) &= \left(\boldsymbol{I} - \sum_{l=1}^{2}\delta_{\nu_{j\ominus 1},l}\boldsymbol{e}_l\boldsymbol{e}_l\right)\cdot\boldsymbol{v}_{j\ominus 1}(\boldsymbol{x},t) \\ &\quad + \sum_{l=1}^{2}\delta_{\nu_{j\ominus 1},l}\boldsymbol{e}_l\left\{\tfrac{1}{2}\left[\boldsymbol{e}_l\cdot\boldsymbol{v}_{j\ominus 1}(\boldsymbol{x}-\boldsymbol{e}_l,t) + \frac{1}{Z}p_{j\ominus 1}(\boldsymbol{x}-\boldsymbol{e}_l,t)\right]\right. \\ &\quad \left. + \tfrac{1}{2}\left[\boldsymbol{e}_l\cdot\boldsymbol{v}_{j\ominus 1}(\boldsymbol{x}+\boldsymbol{e}_l,t) - \frac{1}{Z}p_{j\ominus 1}(\boldsymbol{x}+\boldsymbol{e}_l,t)\right]\right\} \\ &\qquad\qquad (j = 1,\ldots,N) \end{aligned} \tag{10}$$

In this case, the acoustic particle velocity in the $j$th velocity state is a vector quantity

$$\boldsymbol{v}_j(\boldsymbol{x}, t) = \begin{bmatrix} v_{x,j}(\boldsymbol{x}, t) \\ v_{y,j}(\boldsymbol{x}, t) \end{bmatrix} \qquad (j = 1, \ldots, N) \tag{11}$$

Similarly to Eqs. (2) and (3), the acoustic pressure $p(\boldsymbol{x}, t)$ and the acoustic particle velocity $\boldsymbol{v}(\boldsymbol{x}, t)$ of the system are defined by their averages over the velocity states as

$$p(\boldsymbol{x}, t) = \frac{1}{N} \sum_{j=1}^{N} p_j(\boldsymbol{x}, t) \tag{12}$$

and

$$\boldsymbol{v}(\boldsymbol{x}, t) = \frac{1}{N} \sum_{j=1}^{N} \boldsymbol{v}_j(\boldsymbol{x}, t) \tag{13}$$

From the preceding expressions, we can think of our two-dimensional model as a variation of splitting methods.[15] In splitting methods, the temporal evolution of a multidimensional system is generated by applying the time evolution rule of the underlying one-dimensional system to the temporal evolution along each spatial direction in a definite way. In our case, it becomes very easy to incorporate this idea into our model. That is, we have only to reinterpret some of the nonpropagation states of the one-dimensional model as unit speed propagation states along the $y$ axis.

Figure 1 shows an example of the calculation of the temporal evolution of the acoustic pressure using our model. In this calculation, $M = 1$, $N = 2$, $Z = 1$, and the initial condition is

$$p_j(\boldsymbol{x}, 0) = \begin{cases} 10 & (45 \le x \le 54,\ 45 \le y \le 54) \\ 0 & \text{otherwise} \end{cases} \qquad (j = 1, 2) \tag{14}$$

and

$$\boldsymbol{v}_j(\boldsymbol{x}, 0) = \boldsymbol{0} \quad (j = 1, 2) \tag{15}$$

We can see that the wave front moves with speed 1/2.

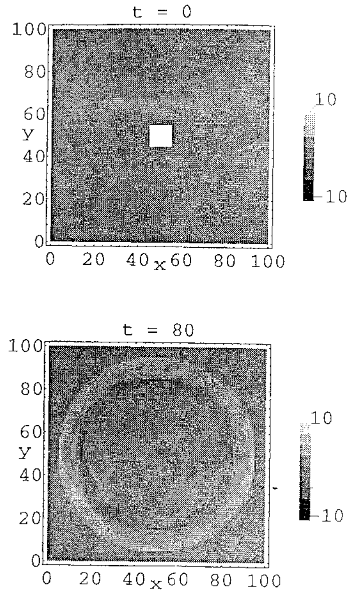


**Fig. 1 Example calculation of the temporal evolution of the acoustic pressure for $C = \frac{1}{2}$.**

**Continuum Limit**

To examine the continuum limit, the sampling distance $\Delta x = \Delta y \equiv \Delta r$ and the sampling time $\Delta t$ are explicitly shown in this subsection. For simplicity, they are assumed to be

$$\Delta r = \epsilon \chi \tag{16}$$

and

$$\Delta t = \epsilon \tau \tag{17}$$

The continuum limit is expressed by $\epsilon \to 0$. Let's expand the field variables in $\epsilon$ as

$$p_j(\boldsymbol{x}, t) = \sum_{l=0}^{\infty} \epsilon^l p_j^{(l)}(\boldsymbol{x}, t) \qquad (j = 1, \ldots, N) \tag{18}$$

$$\boldsymbol{v}_j(\boldsymbol{x}, t) = \sum_{l=0}^{\infty} \epsilon^l \boldsymbol{v}_j^{(l)}(\boldsymbol{x}, t) \qquad (j = 1, \ldots, N) \tag{19}$$

$$p(\boldsymbol{x}, t) = \sum_{l=0}^{\infty} \epsilon^l p^{(l)}(\boldsymbol{x}, t), \tag{20}$$

and

$$\boldsymbol{v}(\boldsymbol{x}, t) = \sum_{l=0}^{\infty} \epsilon^l \boldsymbol{v}^{(l)}(\boldsymbol{x}, t) \tag{21}$$

From Eqs. (12) and (13), $p^{(l)}$ and $p_j^{(l)}$ are related by

$$p^{(l)}(\boldsymbol{x}, t) = \frac{1}{N} \sum_{j=0}^{N} p_j^{(l)}(\boldsymbol{x}, t) \qquad (l = 0, 1, 2, \ldots) \tag{22}$$

and $\boldsymbol{v}^{(l)}$ and $\boldsymbol{v}_j^{(l)}$ by

$$\boldsymbol{v}^{(l)}(\boldsymbol{x}, t) = \frac{1}{N} \sum_{j=0}^{N} \boldsymbol{v}_j^{(l)}(\boldsymbol{x}, t) \qquad (l = 0, 1, 2, \ldots) \tag{23}$$

Using a Taylor series expansion about $\epsilon$, the zeroth-order terms of Eqs. (9) and (10) give

$$p_j^{(0)}(\boldsymbol{x}, t) = p_{j\ominus 1}^{(0)}(\boldsymbol{x}, t) \qquad (j = 1, \ldots, N) \tag{24}$$

and

$$\boldsymbol{v}_j^{(0)}(\boldsymbol{x}, t) = \boldsymbol{v}_{j\ominus 1}^{(0)}(\boldsymbol{x}, t) \qquad (j = 1, \ldots, N) \tag{25}$$

From Eqs. (22) and (23), the preceding equations lead to

$$p^{(0)}(\boldsymbol{x}, t) = p_1^{(0)}(\boldsymbol{x}, t) = \cdots = p_N^{(0)}(\boldsymbol{x}, t) \tag{26}$$

and

$$\boldsymbol{v}^{(0)}(\boldsymbol{x}, t) = \boldsymbol{v}_1^{(0)}(\boldsymbol{x}, t) \cdots = \boldsymbol{v}_N^{(0)}(\boldsymbol{x}, t) \tag{27}$$

Therefore, in the continuum limit, all velocity states become equivalent. Hence, we chose the initial condition Eq. (14) for the calculation of Fig. 1.

The equations for the field variables in the continuum limit can be obtained from the first-order expansion terms of Eqs. (9) and (10). The first-order terms are given by

$$p_j^{(1)}(\boldsymbol{x}, t) + \tau \frac{\partial p_j^{(0)}(\boldsymbol{x}, t)}{\partial t} = p_{j\ominus 1}^{(1)}(\boldsymbol{x}, t) - \chi Z \sum_{l=1}^{2} \delta_{\nu_{j\ominus 1}, l}(\boldsymbol{e}_l \cdot \nabla) \times \boldsymbol{e}_l \cdot \boldsymbol{v}_{j\ominus 1}^{(0)}(\boldsymbol{x}, t) \qquad (j = 1, \ldots, N) \tag{28}$$

and

$$v_j^{(1)}(x,t)+\tau\frac{\partial v_j^{(0)}(x,t)}{\partial t} = v_{j\ominus 1}^{(1)}(x,t)-\frac{\chi}{Z}\sum_{l=1}^{2}\delta_{\nu_{j\ominus 1},l} \times e_l e_l\cdot\nabla p_{j\ominus 1}^{(0)}(x,t) \qquad (j=1,\ldots,N) \tag{29}$$

Summing these equations from $j=1$ to $j=N$ and using Eqs. (22) and (23), one has

$$\tau\frac{\partial p^{(0)}(x,t)}{\partial t}=-\frac{\chi Z}{N}\sum_{j=1}^{N}\sum_{l=1}^{2}\delta_{\nu_j,l}(e_l\cdot\nabla)e_l\cdot v_j^{(0)}(x,t) \tag{30}$$

and

$$\tau\frac{\partial v^{(0)}(x,t)}{\partial t}=-\frac{\chi}{NZ}\sum_{j=1}^{N}\sum_{l=1}^{2}\delta_{\nu_j,l}e_l e_l\cdot\nabla p_j^{(0)}(x,t) \tag{31}$$

From the definition, one has

$$\sum_{l=1}^{2}e_l e_l=I \tag{32}$$

Using Eqs. (8), (26), (27), and (32), Eqs. (30) and (31) become

$$\frac{\partial p^{(0)}(x,t)}{\partial t}=-cZ\nabla\cdot v^{(0)}(x,t) \tag{33}$$

and

$$\frac{\partial v^{(0)}(x,t)}{\partial t}=-\frac{c}{Z}\nabla p^{(0)}(x,t) \tag{34}$$

where $c$ is defined by

$$c\equiv\frac{M\chi}{N\tau}=\frac{M\Delta r}{N\Delta t} \tag{35}$$

These equations are the continuum limit of our model.

If one assumes a linearized adiabatic relation for an equation of state

$$p=c^2\rho \tag{36}$$

and if one interprets $Z$ as a characteristic impedance of the medium

$$Z=\rho_0 c \tag{37}$$

then one can see that Eqs. (33) and (34) are equivalent to the equations of sound in a fluid medium.[16] Hence, one can interpret $p(x,t)$, $v(x,t)$, $\rho(x,t)$, $\rho_0$, and $c$ as the acoustic pressure, the acoustic particle velocity, the acoustic density, the ambient density, and the sound speed of the medium, respectively. Therefore, as a model of sound propagation in fluid media, our model is consistent.

### Condition on the $\nu_j$

The choice of the $\nu_j$ affects the behavior of the two-dimensional lattice gas sound propagation model. This is not restricted to the cases with different values of $C$. A different behavior will be observed for different set values of $M$ and $N$ but the same value of $C$. In this two-dimensional model, the choice of the $\nu_j$ also affects the numerical property of the model. In the one-dimensional lattice gas sound propagation model, there is no truncation error. However, in this two-dimensional model, there are truncation errors. If we require that the first-order truncation error should be zero, we can obtain a condition on the $\nu_j$. In this subsection, using the analysis of the preceding subsection, the equations for the first-order correction terms are examined. Requiring the equations to be the same form as that of the continuum limit, a condition on the $\nu_j$ is obtained. Then we give an example of the $\nu_j$ that satisfies this condition.

The first-order terms of Eqs. (9) and (10) are obtained as Eqs. (28) and (29). We can use Eqs. (26), (27), (33), and (34) for the zeroth-order field variables. Then, using Eqs. (22), (23), and (8), repeated substitution of Eqs. (28) and (29) about the index $j$ leads to

$$p_j^{(1)}(x,t)=p^{(1)}(x,t) +\chi Z\left\{\frac{M(N+2j-1)}{2N}\nabla\cdot v^{(0)}(x,t) -\sum_{l=1}^{2}\left(\sum_{j'=1}^{j}\delta_{\nu_{j'},l}-\delta_{\nu_j,l}+\frac{1}{N}\sum_{j'=1}^{N}j'\delta_{\nu_{j'},l}\right) \times(e_l\cdot\nabla)e_l\cdot v^{(0)}(x,t)\right\} \qquad (j=1,\ldots,N) \tag{38}$$

and

$$v_j^{(1)}(x,t)=v^{(1)}(x,t) +\frac{\chi}{Z}\left\{\frac{M(N+2j-1)}{2N}\nabla p^{(0)}(x,t) -\sum_{l=1}^{2}\left(\sum_{j'=1}^{j}\delta_{\nu_{j'},l}-\delta_{\nu_j,l}+\frac{1}{N}\sum_{j'=1}^{N}j'\delta_{\nu_{j'},l}\right) \times e_l e_l\cdot\nabla p^{(0)}(x,t)\right\} \qquad (j=1,\ldots,N) \tag{39}$$

The second-order terms of Eqs. (9) and (10) give

$$p_j^{(2)}(x,t)+\tau\frac{\partial p^{(1)}(x,t)}{\partial t}+\frac{\tau^2}{2}\frac{\partial^2 p^{(0)}(x,t)}{\partial t^2} = p_{j\ominus 1}^{(2)}(x,t)-\sum_{l=1}^{2}\delta_{\nu_{j\ominus 1},l}\left[\chi Z(e_l\cdot\nabla)e_l\cdot v_{j\ominus 1}^{(1)}(x,t) -\frac{\chi^2}{2}(e_l\cdot\nabla)^2 p_{j\ominus 1}^{(0)}(x,t)\right] \qquad (j=1,\ldots,N) \tag{40}$$

and

$$v_j^{(2)}(x,t)+\tau\frac{\partial v^{(1)}(x,t)}{\partial t}+\frac{\tau^2}{2}\frac{\partial^2 v^{(0)}(x,t)}{\partial t^2} = v_{j\ominus 1}^{(2)}(x,t)-\sum_{l=1}^{2}\delta_{\nu_{j\ominus 1},l}e_l\left[\frac{\chi}{Z}e_l\cdot\nabla p_{j\ominus 1}^{(1)}(x,t) -\frac{\chi^2}{2}(e_l\cdot\nabla)^2 v_j^{(0)}(x,t)\right] \qquad (j=1,\ldots,N) \tag{41}$$

Similarly to the derivation of Eqs. (33) and (34), summing Eqs. (40) and (41) from $j=1$ to $N$ and using the results for the zeroth-order terms, one has

$$\frac{\partial p^{(1)}(x,t)}{\partial t}=-cZ\nabla\cdot v^{(1)}(x,t) \tag{42}$$

and

$$\frac{\partial v^{(1)}(x,t)}{\partial t} =-\frac{c}{Z}\nabla p^{(1)}(x,t)-\frac{\chi^2}{\tau}\sum_{l\neq l'}f_{l,l'}e_l e_{l'}\cdot\frac{\partial^2 v^{(0)}(x,t)}{\partial x\partial y} \tag{43}$$

where the coefficient $f_{l,l'}$ is defined by

$$f_{l,l'} = \frac{M}{N^2}\sum_{j=1}^{N} j\left(\delta_{\nu_j,l} - \delta_{\nu_j,l'}\right)$$

$$-\frac{1}{2N}\sum_{j=1}^{N}\sum_{j'=1}^{j}\left(\delta_{\nu_j,l}\delta_{\nu_{j'},l'} - \delta_{\nu_j,l'}\delta_{\nu_{j'},l}\right) \tag{44}$$

Equation (42) has the same form as Eq. (33). On the other hand, we have an additional term in Eq. (43). This additional term gives the first-order truncation error. To eliminate this correction term, the $\nu_j$ have to satisfy

$$f_{l,l'} = 0 \quad \text{for} \quad l \neq l' \tag{45}$$

This is the condition for our two-dimensional model to be second-order accurate.

An example of the $\nu_j$ that satisfy Eq. (45) is

$$\{\nu_j\} = \{1, \overbrace{0,\ldots,0}^{a_1}, 2, \overbrace{0,\ldots,0}^{b_1}, 1, \overbrace{0,\ldots,0}^{a_2},$$

$$2, \overbrace{0,\ldots,0}^{b_2}, \ldots, 1, \overbrace{0,\ldots,0}^{a_M}, 2, \overbrace{0,\ldots,0}^{b_M}\} \tag{46}$$

where $a_m$ indicates the number of zeros between the $m$th 1 and the following nonzero element, and $b_m$ does that between the $m$th 2 and the following nonzero element. The number of zeros is assumed to satisfy

$$\sum_{m=1}^{M} a_m = \sum_{m=1}^{M} b_m = \frac{N-2M}{2} \tag{47}$$

Therefore the total number of zeros in $\{\nu_j\}$ needs to be an even integer. An example of these $\nu_j$ for $N = 6$ and $M = 2$ is

$$\{\nu_j\} = \{1, 0, 2, 1, 2, 0\} \tag{48}$$

Figures 2 and 3 show the effect of the choice of the $\nu_j$ on the temporal evolution of pressure and intensity. In this calculation, $M = 1$, $N = 4$, and $Z = 1$, and the initial conditions are

$$p_j(\boldsymbol{x}, 0) = \begin{cases} 10 & \text{for } \boldsymbol{x} = (6, 6) \\ 0 & \text{otherwise} \end{cases} \quad (j = 1, \ldots, N) \tag{49}$$

and

$$\boldsymbol{v}_j(\boldsymbol{x}, 0) = \boldsymbol{0} \qquad (j = 1, \ldots, N) \tag{50}$$

We have seen that all velocity states become equivalent in the continuum limit. Hence, the initial condition is also taken to satisfy this limit. The instantaneous intensity is defined as

$$\boldsymbol{I}(\boldsymbol{x}, t) \equiv \frac{1}{N}\sum_{j=1}^{N} p_j(\boldsymbol{x}, t)\boldsymbol{v}_j(\boldsymbol{x}, t) \tag{51}$$

From these figures, one can see that there are little differences in the temporal change of pressure. However, the temporal evolutions of intensity are apparently different for the two $\{\nu_j\}$. The intensity field for $\{\nu_j\} = \{1, 0, 2, 0\}$, which satisfies Eq. (45), shows the same rotational symmetry as that of the lattice. For $\{\nu_j\} = \{1, 0, 0, 2\}$, which does not satisfy the condition, the intensity field is not symmetric compared with the lattice. This result corresponds to the relation that the first-order truncation error appears in the equation for $\boldsymbol{v}(\boldsymbol{x}, t)$ but not in that for $p(\boldsymbol{x}, t)$.

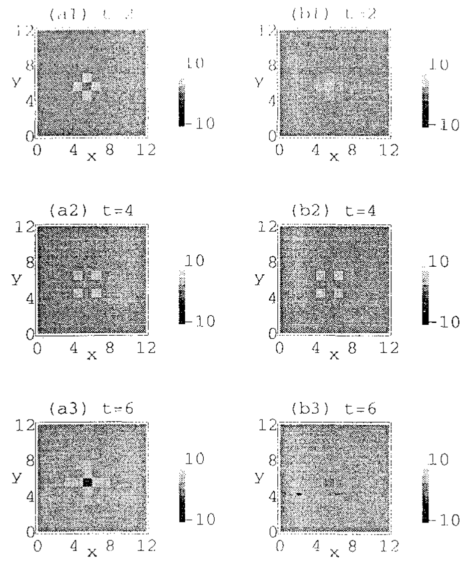


**Fig. 2 Temporal evolution of pressure for two different $\nu_j$. a1–a3: $\{\nu_j\} = \{1, 0, 2, 0\}$, and b1–b3: $\{\nu_j\} = \{1, 0, 0, 2\}$.**

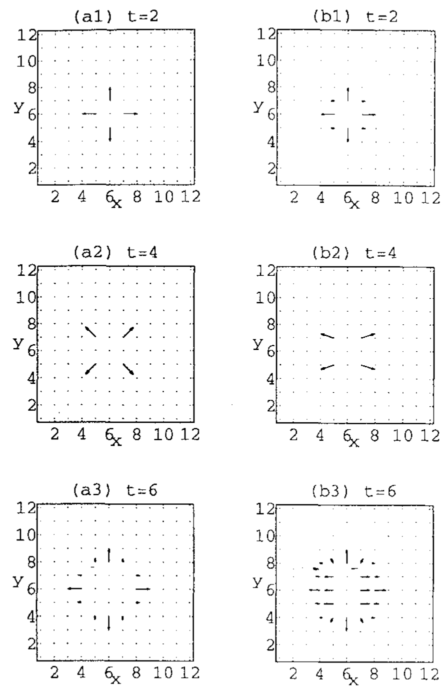


**Fig. 3 Temporal evolution of intensity for two different $\nu_j$. a1–a3: $\{\nu_j\} = \{1, 0, 2, 0\}$, and b1–b3: $\{\nu_j\} = \{1, 0, 0, 2\}$.**

### von Neumann Stability Analysis

In this subsection using the $\nu_j$ of Eq. (46), we apply a von Neumann stability analysis to our model.[17] This Fourier analysis gives us the dispersion relation, the group velocity, and the stability of our model.

Substituting $p_j(\boldsymbol{x}, t) = \hat{p}_j \exp\{i(\boldsymbol{k}\cdot\boldsymbol{x} - \omega t)\}$ and $\boldsymbol{v}_j(\boldsymbol{x}, t) = \hat{\boldsymbol{v}}_j \exp\{i(\boldsymbol{k}\cdot\boldsymbol{x} - \omega t)\}$ into Eqs. (9) and (10), one has

$$e^{-i\omega}\begin{pmatrix}\hat{p}_j \\ \hat{v}_{x,j} \\ \hat{v}_{y,j}\end{pmatrix} = \boldsymbol{Z}^{-1}\left\{\sum_{l=0}^{2}\delta_{\nu_{j\ominus 1},l}\boldsymbol{U}_l\right\}$$

$$\times\boldsymbol{Z}\begin{pmatrix}\hat{p}_{j\ominus 1} \\ \hat{v}_{x,j\ominus 1} \\ \hat{v}_{y,j\ominus 1}\end{pmatrix} \qquad (j = 1, \ldots, N) \tag{52}$$

where the matrices $\boldsymbol{Z}$ and $\boldsymbol{U}_l$ are defined as

$$\boldsymbol{Z} = \begin{pmatrix} 1 & 0 & 0 \\ 0 & Z & 0 \\ 0 & 0 & Z \end{pmatrix} \tag{53}$$

$$\boldsymbol{U}_0 = \begin{pmatrix} 1 & 0 & 0 \\ 0 & 1 & 0 \\ 0 & 0 & 1 \end{pmatrix} (\equiv \boldsymbol{I}) \tag{54}$$

$$\boldsymbol{U}_1 = \begin{pmatrix} \cos k_x & -i\sin k_x & 0 \\ -i\sin k_x & \cos k_x & 0 \\ 0 & 0 & 1 \end{pmatrix} \tag{55}$$

and

$$\boldsymbol{U}_2 = \begin{pmatrix} \cos k_y & 0 & -i\sin k_y \\ 0 & 1 & 0 \\ -i\sin k_y & 0 & \cos k_y \end{pmatrix} \tag{56}$$

Substituting Eq. (52) into the right-hand side repeatedly, one can obtain an equation for $(\hat{p}_j, \hat{v}_{x,j}, \hat{v}_{y,j})$. From the definition of the $\nu_j$ of Eq. (46), this repeated substitution leads to the two matrix equations

$$e^{-iN\omega}\begin{pmatrix} \hat{p}_j \\ \hat{v}_{x,j} \\ \hat{v}_{y,j} \end{pmatrix} = \boldsymbol{Z}^{-1}\begin{Bmatrix} \boldsymbol{U}^M \\ \left(\boldsymbol{U}^{\mathrm{T}}\right)^M \end{Bmatrix}\boldsymbol{Z}\begin{pmatrix} \hat{p}_j \\ \hat{v}_{x,j} \\ \hat{v}_{y,j} \end{pmatrix}$$

$$\text{for } \begin{Bmatrix} j \in N_1 \\ j \in N_2 \end{Bmatrix} \tag{57}$$

where the matrix $\boldsymbol{U}$ is defined by

$$\boldsymbol{U} = \boldsymbol{U}_1\boldsymbol{U}_2 = \begin{pmatrix} \cos k_x \cos k_y & -i\sin k_x & -i\cos k_x \sin k_y \\ -i\sin k_x \cos k_y & \cos k_x & -\sin k_x \sin k_y \\ -i\sin k_y & 0 & \cos k_y \end{pmatrix} \tag{58}$$

and the superscript $T$ means a transposition of the matrix. The two sets of indices $N_1$ and $N_2$ are defined by

$$N_1 = \{j \mid \text{when decreasing } j \text{ one by one using “}\ominus\text{,” the first nonzero } \nu_{j'} \text{ is } 1\} \tag{59}$$

and

$$N_2 = \{j \mid \text{when decreasing } j \text{ one by one using “}\ominus\text{,” the first nonzero } \nu_{j'} \text{ is } 2\} \tag{60}$$

For example, when $\{\nu_j\} = \{1, 0, 2, 0\}$, this definition gives $N_1 = \{2, 3\}$ and $N_2 = \{1, 4\}$.

From Eq. (57), the dispersion relation of the system is obtained as

$$e^{-iN\omega} = 1, e^{iM\beta}, \quad \text{and} \quad e^{-iM\beta} \tag{61}$$

where 1 and $e^{\pm i\beta}$ are the eigenvalues of the matrix $\boldsymbol{U}$ and $\beta$ is defined by

$$\beta = \mathrm{Arccos}\left(\frac{\cos k_x \cos k_y + \cos k_x + \cos k_y - 1}{2}\right) \tag{62}$$

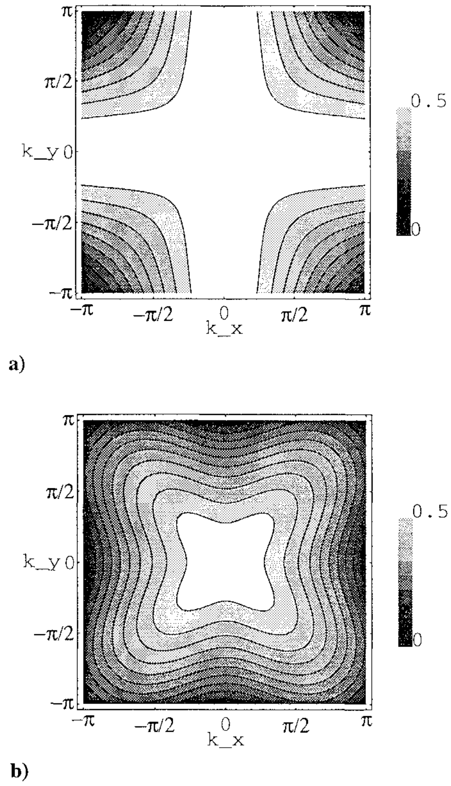


**Fig. 4 Group velocity for two different discrete two-dimensional wave models: a) our model [Eq. (63)] with $M = 1$ and $N = 2$ and b) a finite difference model of Eq. (64) with $C = \frac{1}{2}$.**

For real valued $k_x$ and $k_y$, the right-hand side of Eq. (62) is always real valued and the magnitude is less than or equal to one. Hence, $\beta$ is always real valued for real valued $k_x$ and $k_y$. Then the magnitude of the right-hand side of Eq. (61) is always one. This means that the system is stable.

Differentiating Eq. (61) with respect to $k$, we can obtain the group velocity of the system. For $e^{-iN\omega} = 1$, the group velocity becomes zero. This corresponds to a spurious wave such as those seen in nondissipative finite difference schemes. For the other cases, we have

$$c_g = \pm\frac{M\left[k_x \sin k_x \cos^2(k_y/2) + k_y \sin k_y \cos^2(k_x/2)\right]}{Nk\sqrt{1 - \frac{1}{4}(\cos k_x \cos k_y + \cos k_x \cos k_y - 1)^2}} \tag{63}$$

Figure 4 shows the behavior of the nonzero group velocity against the nondimensionalized wave number. In this figure the group velocity for a finite difference model of wave equation is also shown. This finite difference model is expressed by

$$\begin{aligned} &p(\boldsymbol{x}, t+1) - 2p(\boldsymbol{x}, t) + p(\boldsymbol{x}, t-1) \\ &\quad = C^2\{[p(\boldsymbol{x}+\boldsymbol{e}_1, t) - 2p(\boldsymbol{x}, t) + p(\boldsymbol{x}-\boldsymbol{e}_1, t)] \\ &\quad + [p(\boldsymbol{x}+\boldsymbol{e}_2, t) - 2p(\boldsymbol{x}, t) + p(\boldsymbol{x}-\boldsymbol{e}_2, t)]\} \end{aligned} \tag{64}$$

which can be obtained by applying the second-order central difference to a two-dimensional wave equation. The group velocity of the continuum model is 1/2 and is independent of wave number. In the finite difference model, the group velocity is close to the continuum case for the small wave number region. In our two-dimensional model, the correct group velocity region is extended along the $x$ axis and the $y$ axis. This suggests that the two-dimensional model is a good approximation for narrow angle propagations along the coordinate axes. In the next subsection, we examine this relation.

**Narrow Angle Propagation**

To analyze the behavior of our model for narrow angle propagations, the continuum limit and the small angle expansion of the Fourier representation is considered. Using the cylindrical coordinate system in the wave number space, $k_x$ and $k_y$ are expressed as

$$k_x = k\cos\theta \tag{65}$$

and

$$k_y = k\sin\theta \tag{66}$$

Small angle propagations along the $x$ axis are expressed using $\Delta\theta \ll 1$, where $\Delta\theta$ expresses the order of the important region of $\theta$ in the wave number space.

In the continuum limit only the dispersion relation that satisfies $\omega \to 0$ for $|\boldsymbol{k}| \to 0$ becomes important. Therefore, in the continuum limit, the factors of both sides of Eq. (57) may be reduced by their principal logarithm. Hence, Eq. (57) is reduced to

$$-iN\omega\Delta t\begin{pmatrix}\hat{p}_j\\ \hat{v}_{x,j}\\ \hat{v}_{y,j}\end{pmatrix} = \boldsymbol{M}\left\{\begin{matrix}\mathrm{Log}(\boldsymbol{Z}^{-1}\boldsymbol{U}\boldsymbol{Z})\\ \mathrm{Log}\left[(\boldsymbol{Z}^{-1}\boldsymbol{U}\boldsymbol{Z})^{\mathrm{T}}\right]\end{matrix}\right\}\begin{pmatrix}\hat{p}_j\\ \hat{v}_{x,j}\\ \hat{v}_{y,j}\end{pmatrix}$$

$$\text{for}\quad \left\{\begin{matrix} j\in N_1\\ j\in N_2\end{matrix}\right\} \tag{67}$$

In this subsection, $\Delta r$ and $\Delta t$ are explicitly shown.

Since $\boldsymbol{U}$ is a unitary matrix with eigenvalues 1 and $e^{\pm i\beta}$, using an appropriate unitary matrix $\boldsymbol{V}$, it can be expressed as

$$\boldsymbol{U} = \exp\left\{i\beta\boldsymbol{V}\begin{pmatrix}0&0&0\\0&1&0\\0&0&-1\end{pmatrix}\boldsymbol{V}^\dagger\right\} \tag{68}$$

where $\dagger$ means a Hermite conjugate (transpose conjugate) of the matrix. Using a Taylor series expansion about $\theta$ and $\epsilon$, one has

$$\mathrm{Log}\,\boldsymbol{Z}^{-1}\boldsymbol{U}\boldsymbol{Z} = i\beta\boldsymbol{Z}^{-1}\boldsymbol{V}\begin{pmatrix}0&0&0\\0&1&0\\0&0&-1\end{pmatrix}\boldsymbol{V}^\dagger\boldsymbol{Z}$$

$$= \boldsymbol{Z}^{-1}\begin{pmatrix}0 & -ik_x\Delta r & -ik_y\Delta r\\ -ik_x\Delta r & 0 & -k^2\theta\Delta r^2/2\\ -ik_y\Delta r & -k^2\theta\Delta r^2/2 & 0\end{pmatrix}\boldsymbol{Z}$$

$$+\,\mathcal{O}(\theta\Delta r^3) \tag{69}$$

Substituting Eq. (69) into Eq. (67) and taking a summation from $j = 1$ to $N$, one has

$$-\,i\omega\hat{p} = -cZi\boldsymbol{k}\cdot\hat{\boldsymbol{v}} + \mathcal{O}(\theta\Delta r^2) \tag{70}$$

$$-i\omega\hat{v}_x = -\frac{c}{Z}ik_x\hat{p} - \frac{k^2c}{2N}\theta\Delta r$$

$$\times\left(\sum_{j\in N_1}\hat{v}_{y,j} - \sum_{j\in N_2}\hat{v}_{y,j}\right) + \mathcal{O}(\theta\Delta r^2) \tag{71}$$

and

$$-i\omega\hat{v}_y = -\frac{c}{Z}ik_y\hat{p} + \frac{k^2c}{2N}\theta\Delta r$$

$$\times\left(\sum_{j\in N_1}\hat{v}_{x,j} - \sum_{j\in N_2}\hat{v}_{x,j}\right) + \mathcal{O}(\theta\Delta r^2) \tag{72}$$

Applying a Taylor series expansion about $\theta$ and $\epsilon$ to Eq. (52), and using a similar discussion to the derivation of Eqs. (38) and (39), one has

$$\begin{pmatrix}\hat{p}_j\\ \hat{v}_{x,j}\\ \hat{v}_{y,j}\end{pmatrix} = \begin{pmatrix}\hat{p}\\ \hat{v}_x\\ \hat{v}_y\end{pmatrix} + \mathcal{O}(\Delta r)\quad (j = 1,\ldots,N) \tag{73}$$

From this equation, Eqs. (71) and (72) are reduced to

$$-\,i\omega\hat{\boldsymbol{v}} = -\frac{c}{Z}i\boldsymbol{k}\hat{p} + \mathcal{O}(\theta\Delta r^2) \tag{74}$$

Since an inverse Fourier transform includes an integral over $\theta$, one has

$$\mathcal{F}^{-1}[\mathcal{O}(\theta^n)] = \mathcal{O}(\Delta\theta^{n+1}) \tag{75}$$

Therefore, applying an inverse Fourier transform to Eqs. (70) and (74), one has

$$\frac{\partial p(\boldsymbol{x},t)}{\partial t} = -cZ\nabla\cdot\boldsymbol{v}(\boldsymbol{x},t) + \mathcal{O}(\Delta\theta^2\Delta r^2) \tag{76}$$

and

$$\frac{\partial \boldsymbol{v}(\boldsymbol{x},t)}{\partial t} = -\frac{c}{Z}\nabla p(\boldsymbol{x},t) + \mathcal{O}(\Delta\theta^2\Delta r^2) \tag{77}$$

Therefore the narrower the angle of propagations becomes, the more the truncation error is decreased.

## Conclusions

We have developed a method to extend our one-dimensional sound propagation model to a two-dimensional square lattice. From an analysis of the continuum limit, we have obtained the condition for the model to be second-order accurate. A von Neumann analysis has shown that our model is stable and has an anisotropic dispersion. The group velocity shows that the truncation error of our model becomes smaller as the propagation angle from the coordinate axes decreases. In fact, for propagation directly along the coordinate axes, there is no dispersion or truncation error.

Although there is no room to describe it here, we have obtained the following additional extensions to our lattice gas sound propagation model: Using the methods explained in this paper, we have made a sound propagation model in a two-dimensional hexagonal lattice. It is also found that dissipation effects can be included. In the formulation of this paper, the wave speed values $\nu_j$ are a time-independent function. If we introduce a time-dependent $\{\nu_j\}$, we can reduce the number of the velocity states. This formulation reduces the amount of computer memory to perform a calculation. If we introduce a dependence of $\{\nu_j\}$ on the field variable, we can model a fluid dynamic convection term. These studies will be discussed thoroughly in the near future.

## References

[1]Wolfram, S., "Cellular Automaton Fluids 1: Basic Theory," *Journal of Statistical Physics*, Vol. 45, Nos. 3/4, 1986, pp. 471–526.

[2]Frisch, U., d'Humières, D., Hasslacher, B., Lallemand, P., Pomeau, Y., and Rivet, J., "Lattice Gas Hydrodynamics in Two and Three Dimensions," *Complex Systems*, Vol. 1, No. 4, 1987, pp. 649–707.

[3]Doolen, G. D., Frisch, U., Hasslacher, B., Orszag, S., and Wolfram, S. (eds.), *Lattice Gas Methods for Partial Differential Equations*, Addison–Wesley, Redwood City, CA, 1990.

[4]Manneville, P., Boccara, N., Vichniac, G. Y., and Bidaux, R. (eds.), *Cellular Automata and Modeling of Complex Physical Systems*, Springer–Verlag, Berlin, 1989.

[5]Doolen, G. D. (ed.), *Lattice Gas Methods: Theory, Applications, and Hardware*, MIT Press, Cambridge, MA, 1991.

[6]Margolus, N., Toffoli, T., and Vichniac, G., "Cellular-Automata Supercomputers for Fluid-Dynamics Modeling," *Physical Review Letters*, Vol. 56, No. 16, 1986, pp. 1694–1696.

[7]Rothman, D. H., "Modeling Seismic *P*-Waves with Cellular Automata," *Geophysical Research Letters*, Vol. 14, No. 1, 1987, pp. 17–20.

[8]Huang, J., Chu, Y., and Yin, C., "Lattice-Gas Automata for Modeling Acoustic Wave Propagation in Inhomogeneous Media," *Geophysical Research Letters*, Vol. 15, No. 11, 1988, pp. 1239–1241.

[9]Chen, H., Chen, S., and Doolen, G. D., "Sound Wave Propagation in FHP Lattice Gas Automata," *Physics Letters A*, Vol. 140, No. 4, 1989, pp. 161–165.

[10]Lavallée, P., "Attenuation of Sound Waves in Lattice Gases," *Physics Letters A*, Vol. 163, Nos. 5/6, 1992, pp. 392–396.

[11]Chen, H., Chen, S., Doolen, G., and Lee, Y. C., "Simple Lattice Gas Models for Waves," *Complex Systems*, Vol. 2, No. 3, 1988, pp. 259–267.

[12]Krutar, R. A., Numrich, S. K., Squier, R. K., Pearson, J., and Doolen, G., "Computation of Acoustic Field Behavior Using a Lattice Gas Model," *IEEE Ocean Technologies and Opportunities in the Pacific for the 90's*, Inst. of Electrical and Electronics Engineers, Piscataway, NJ, 1991, pp. 447–452.

[13]Numrich, S. K., Krutar, R. A., and Squier, R., "Computation of Acoustic Fields on a Massively Parallel Processor Using Lattice Gas Methods," *Computational Acoustics*, edited by R. L. Lau, D. Lee, and A. R. Robinson, Vol. 1, North-Holland, Amsterdam, 1993, pp. 81–92.

[14]Sudo, Y., and Sparrow, V. W., "A New Lattice Gas Model for 1-D Sound Propagation," *Journal of Computational Acoustics*, Vol. 1, No. 4, 1993, pp. 423–454.

[15]LeVeque, R. J., *Numerical Methods for Conservation Laws*, Birhäuser Verlag, Basel, 1990, pp. 202–205.

[16]Pierce, A. D., *Acoustics: An Introduction to Its Physical Principles and Applications*, Acoustical Society of America, Woodbury, New York, 1989.

[17]Hirsch, C., *Numerical Computation of Internal and External Flows, Fundamentals of Numerical Discretization*, Vol. 1, Wiley, Chichester, England, UK, 1988.